

Search-based Software Testing Driven by Automatically Generated and Manually Defined Fitness Functions

Federico Formica
formicaf@mcmaster.ca
McMaster University
Hamilton, Ontario, Canada

Mehrnoosh Askarpour
askarpom@mcmaster.ca
McMaster University
Hamilton, Ontario, Canada

Claudio Menghi
menghic@mcmaster.ca
McMaster University
Hamilton, Ontario, Canada

ABSTRACT

Search-based software testing (SBST) typically relies on fitness functions to guide the search exploration toward software failures. There are two main techniques to define fitness functions: (a) automated fitness function computation from the specification of the system requirements and (b) manual fitness function design. Both techniques have advantages. The former uses information from the system requirements to guide the search toward portions of the input domain that are more likely to contain failures. The latter uses the engineers' domain knowledge.

We propose ATheNA, a novel SBST framework that combines fitness functions that are automatically generated from requirements specifications and manually defined by engineers. We design and implement ATheNA-S, an instance of ATheNA that targets Simulink® models. We evaluate ATheNA-S by considering a large set of models and requirements from different domains. We compare our solution with an SBST baseline tool that supports automatically generated fitness functions, and another one that supports manually defined fitness functions. Our results show that ATheNA-S generates more failure-revealing test cases than the baseline tools and that the difference between the performance of ATheNA-S and the baseline tools is not statistically significant. We also assess whether ATheNA-S could generate failure-revealing test cases when applied to a large case study from the automotive domain. Our results show that ATheNA-S successfully revealed a requirement violation in our case study.

KEYWORDS

Testing, Falsification, Fitness Functions, CPS

1 INTRODUCTION

Software failures in cyber-physical systems (CPS) can have *catastrophic and costly consequences*. For example, automotive software failures led to severe injuries and the loss of human lives (e.g., [40, 88, 91]). Car manufacturers had to recall their vehicles, causing reputation damage and millions of U.S. Dollars lost (e.g., [40, 45, 54, 77, 78, 87, 89]).

To prevent these scenarios, CPS engineers extensively test their systems to *detect safety-critical software failures* [8, 29, 38, 99]. This activity is facilitated by automated testing tools (e.g., [4, 10, 62, 67]) that are regularly used in safety critical CPS domains, including automotive (e.g., [62]), aerospace (e.g., [67]), and medical (e.g., [57]).

Automated testing often (e.g., [67]) relies on *search-based software testing* (SBST). SBST iteratively generates test cases until a software failure is detected or the SBST framework exceeds the time budget allotted for the testing activity. Different techniques were studied to build effective SBST frameworks that proposed

the usage of different (a) optimization algorithms (e.g., [23, 59]), (b) input types (e.g., [76]), (c) surrogate models (e.g., [67]), and (d) fitness functions (e.g., [62]). We focus on the fitness function design, a challenging task for designing effective SBST frameworks ([5, 7, 12, 19, 79–81, 95]).

Fitness functions guide SBST frameworks in generating new test cases. They provide metrics (a.k.a. fitness values) that estimate how close the test cases are to detecting a failure [42]. To effectively and efficiently generating failure-revealing test cases, it is critical to select appropriate fitness functions [12, 19, 80, 95]. The fitness function design is usually supported by fitness landscape analysis activities (e.g. [5, 52, 75]) that evaluate how the fitness value changes over the search space. Fitness landscape analysis can help understand the search process and its probability of success (e.g. [44, 51, 52]). However, despite the breadth and diversity of testing domains and solutions, the fitness functions design is still complex and time-consuming (e.g., [7, 9, 81]).

There are two mainstream techniques to define fitness functions: *automated generation* and *manual definition*.

Automated generation of the fitness function (e.g., [14, 27, 34, 56, 66, 73, 92]) derives the fitness function from other artifacts without any human intervention. For example, many SBST frameworks (e.g., [10, 32, 67, 93]) use fitness functions to compute the robustness values derived from temporal logic specifications expressing system requirements (e.g., [34, 41, 68, 73]). These functions typically use the requirement structure to guide the search toward portions of the input domain that are more likely to lead to system failures. Automatically generated fitness functions support SBST in the detection of failures (e.g., [14, 27, 41, 92]), were used to detect failures in industrial models (e.g., [47, 67]), and are used within international tool competitions (e.g., [33]). They are *general purpose*. However, they typically do not use engineers' domain knowledge for the fitness value computation.

Unlike the automated approach, *manual fitness function definition* (e.g., [4, 20, 61, 63, 95]) requires engineers to design the fitness functions using their experience and domain knowledge. For example, engineers can manually define fitness functions to guide the search toward the generation of inputs that are more likely to show the violation of liveness, stability, smoothness, and responsiveness requirements [62]. Manually defined fitness functions effectively and efficiently support SBST: they enable the detection of failures that domain experts could not find by manual testing (e.g., [62]). Manual fitness function design enables engineers to write *model-specific* fitness functions that guide the search toward specific areas of the input domain that are more likely to contain failures, e.g., the boundaries of the input domain. However, in some cases, manually

defined fitness functions are biased and may concentrate the search on areas of the input domains that do not contain failures.

This work proposes ATheNA (AuTomatic-maNuAl) search-based testing, a novel SBST framework driven by automatically generated and manually defined fitness functions. ATheNA combines the benefits of automatically generated and manually defined fitness functions: it exploits both the structure of the requirements and the engineers' domain knowledge to guide the search toward specific areas of the input domain that are likely to reveal software failures. In addition, we define ATheNA-S, an instance of ATheNA that supports Simulink® models. We consider Simulink® models since they are widely-used for specifying the behavior of CPSs in a variety of domains including [21, 55], automotive [62], energy [47] and medical [82]. We implement ATheNA-S as a plugin for S-Taliro [10], a well-known SBST framework for Simulink® models recently classified as ready for industrial usage [48].

We evaluate the effectiveness and efficiency of ATheNA-S in generating failure-revealing test cases. We compare ATheNA-S with S-Taliro [10], a tool that supports automatically generated fitness functions, and ATheNA-SM, a customization of ATheNA-S that supports manually defined fitness functions. We consider seven models and 27 requirements from ARCH 2021 [11, 33], an international SBST competition for Simulink® models that is held as a part of the international conference on computer safety, reliability, and security (SAFECOMP) [1]. For each requirement, we considered a set of assumptions for the inputs of the model. In total, we compare the tools by considering 39 assumption-requirement combinations. Our results show that (a) ATheNA-S performs better than the baseline tools for $\approx 79\%$ of our assumption-requirement combinations, (b) ATheNA-S generates more failure-revealing test cases than S-Taliro (+6.3%) and ATheNA-SM (+8.6%), and (c) the difference between the performance of ATheNA-S and the baseline tools is not statistically significant. Additionally, we assess how applicable and useful is ATheNA-S in generating failure-revealing test cases for a large Simulink® model. We consider the Simulink® model of an electrical automotive software control system [18] developed as a part of the EcoCAR Mobility Challenge [30], a competition sponsored by the U.S. Department of Energy [25], General Motors [39], and MathWorks [60], and use the insights of a lead engineer in a large automotive company to inject a practical fault in the model. We evaluate whether ATheNA-S could generate any failure-revealing test cases. Our results show that ATheNA-S could generate a failure-revealing test within practical time limits.

To summarize, our contributions are:

- We propose the ATheNA framework (Section 2);
- We define ATheNA-S, an instance of ATheNA that supports Simulink® models (Section 3);
- We implement ATheNA-S as a plugin for S-Taliro (Section 4);
- We empirically assess the benefits of ATheNA (Section 5);
- We discuss the impact of our findings on the software engineering practice (Section 6).

This work is organized as follows. Section 2 presents ATheNA. Section 3 describes the instance of ATheNA that targets Simulink® models. Section 4 provides implementation details. Section 5 empirically assesses our contribution. Section 6 discusses our findings

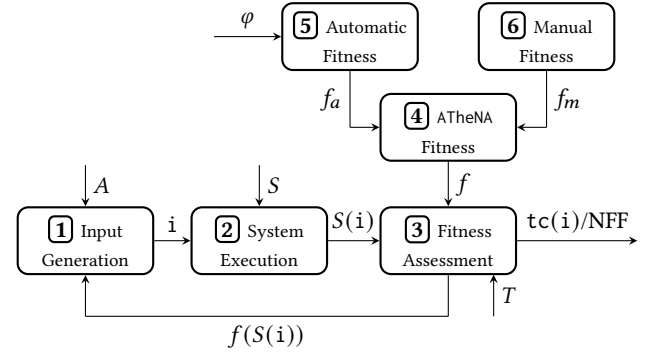


Figure 1: Overview of the ATheNA testing framework.

and presents threats to validity. Section 7 presents related work. Section 8 concludes the work.

2 AUTOMATIC-MANUAL SBST

Figure 1 provides an overview of the ATheNA (AuTomatic-maNuAl) search-based testing framework. Squared boxes report the steps of ATheNA. Incoming and outgoing arrows describe the inputs and outputs of the different steps. Arrows with no source represent the inputs of the ATheNA framework. Arrows with no destination represent the outputs of the ATheNA framework. Arrows connecting two boxes link subsequent steps.

ATheNA has four inputs: a model of the system to be tested (S); an assumption on the system inputs (A), a time budget (T), and a requirement (φ). The output of ATheNA is a failure-revealing test case ($tc(i)$) or an indication that no failure-revealing test case was found (NFF — No Failure Found) within the time budget.

To detect a failure-revealing test case, ATheNA iteratively repeats the steps presented in figure 1:

- **Input Generation (1)**. It generates an input (i) for the system model (S) that satisfies the assumption (A);
- **System Execution (2)**. It runs the system model (S) with the generated input (i) and obtains a system execution ($S(i)$).
- **Fitness Assessment (3)**. It computes the fitness value ($f(S(i))$) associated with the obtained system execution ($S(i)$) and assesses whether the fitness value is below a threshold value.

A test case ($tc(i)$) associated with the input (i) is failure-revealing if: (a) the input satisfies the assumption (A), i.e., $i \models A$, and (b) the fitness value ($f(S(i))$) is smaller than a threshold value (typically the value 0).

The ATheNA framework terminates when a failure-revealing test case ($tc(i)$) is detected or when the framework exceeds the time budget (T) without finding any failure-revealing test case. For the former case, ATheNA returns the failure-revealing test case. For the latter case, ATheNA returns the NFF value.

The fitness value ($f(S(i))$) is used to guide the ATheNA framework. The search algorithm tries to find an input that minimizes the fitness value. To reach this goal, it uses the fitness value computed in step 3 to drive the generation of the next input (1).

To compute the fitness value, ATheNA combines manually defined and automatically generated fitness functions and has the following steps:

- **AThENA Fitness (4)**. It returns a fitness function (f) that combines the values computed by the manually defined and automatically generated fitness functions. Depending on the testing necessities, the fitness function f can prioritize one of the two values. The function can also change the prioritization policy dynamically during the search if the fitness value is not effectively guiding the SBST framework.
- **Automatic Fitness (5)**. It returns a fitness function (f_a) automatically generated from requirement φ . The requirement is automatically compiled into a function that, given a system execution $S(i)$, computes a fitness value (f_a).
- **Manual Fitness (6)**. It returns a fitness function (f_m) manually defined by the engineers. It computes a fitness value for the system execution $S(i)$.

ATheNA can be instantiated by considering different modeling formalisms. One possible instance of ATheNA is presented in the next section.

3 AUTOMATIC-MANUAL SBST FOR SIMULINK®

This section describes ATheNA-S, an instance of ATheNA that supports Simulink[®], a graphical language for model design.

Figure 2 presents our running example: the variation of the Automatic Transmission (AT) model provided by Mathworks [16], used in the applied verification for continuous and hybrid systems competition [11, 33].

Simulink® provides visual constructs to design a system model (S). *Blocks* typically represent operations and constant values. They are aggregated into subsystems labeled with *ports* that identify the inputs and outputs of the subsystems. For example, Engine is one of the subsystems of the Simulink® model of figure 2. It has two input ports (Ti and Throttle) and one output port (Ne). *Connections* link input and output ports. For example, a connection links the output port NE of the Engine subsystem to the input port NE of the Transmission subsystem. The inputs and outputs of a Simulink® model are represented by the *inports* and *outports* blocks. For example, in figure 2, there are two inputs (Throttle, and Brake) and three outputs (Speed, RPM, and Gear).

We instantiated ATheNA to support Simulink® models as follows.

Input Generation (1). The input generation step generates a set of signals $\mathbf{i} = \{i_1, i_2, \dots, i_m\}$, one per inport. For example, for the AT model, ATheNA generates the input signals for the `Throttle` and `Brake` inports. Let $\mathbb{T} = [0, b]$ be a non-singular bounded interval of \mathbb{R} representing the simulation time domain of system S , a signal is a function $f : \mathbb{T} \rightarrow \mathbb{R}$. The Simulink® simulator requires engineers to specify the input of the simulation. Figure 3a presents an example of an input for the AT model. The input contains the two input signals for the `Throttle` and `Brake` inports defined over the simulation time domain $[0, 50]$ s.

Assumption A guides the generation of new input signals. For each input signal $i_i \in \mathbf{i}$, it contains a triple $\langle int_i, R_i, n_i \rangle$ made of an interpolation function (int_i), a value range (R_i) and a number of control points. ATheNA-S generates each input signal i_i by selecting

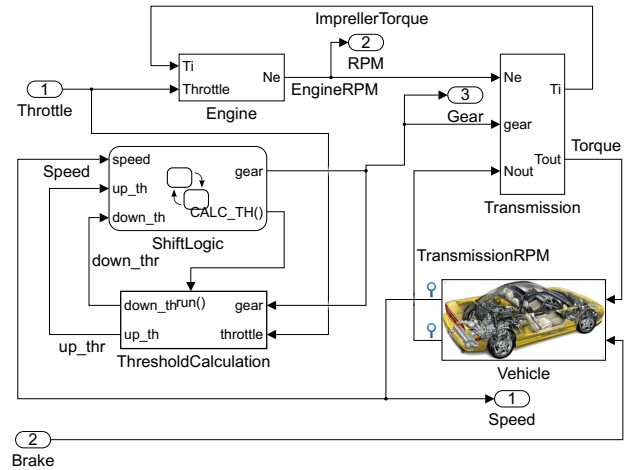


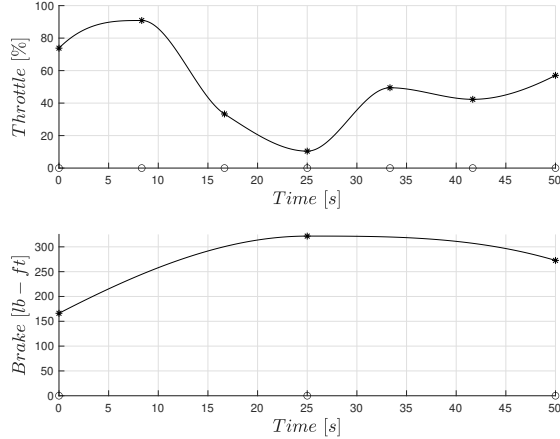
Figure 2: Simulink® model of the AT example.

n_i time instants, i.e., t_1, t_2, \dots, t_{n_i} , within the time domain $T = [0, b]$, such that $t_1 = 0$, $t_{n_i} = b$ and $t_1 < t_2 < \dots < t_{n_i}$. The values of t_1, t_2, \dots, t_{n_i} can also be chosen to ensure a fixed difference between consecutive time instants, i.e., for all t_j, t_{j+1} with $j \in \{1, 2, \dots, n_i - 1\}$, the value of $t_{j+1} - t_j$ is fixed. Then, ATHeNA-S selects a value $i_i(t_j)$ from value range R_i for each time instant t_j . The interpolation function (e.g., piecewise constant, linear or piecewise cubic) is then used to generate the values assumed by input signal i_i over the rest of time domain T . For example, the input signals for the Throttle and Brake reported in figure 3a are generated by considering the value range $[0, 100]$ for the throttle percentage applied to the engine (%), and $[0, 325]$ for the pound-foot (lb - ft) torque applied by the brake. To generate the input signals, 10 control points and the Piecewise Cubic Hermite Interpolating Polynomial (pchip) interpolation function [74] are considered. The values selected for the time instants are indicated in the figure 3a with the “o” symbol on the x-axis. The points on the input signals labeled with the “*” symbol indicate the values selected for the input signals at these time instants.

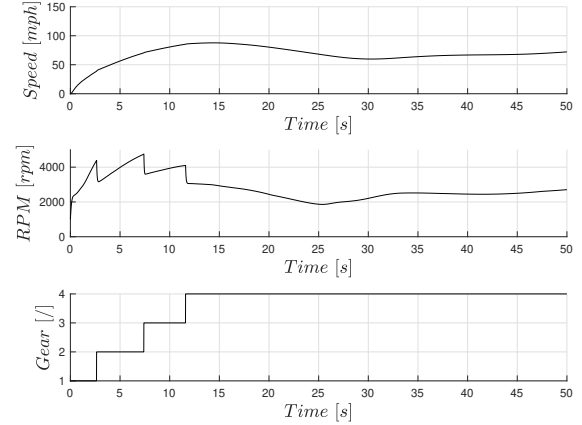
System Execution (2). ATHeNA-S uses the Simulink® simulator to execute system S for input i and to produce output o , i.e., $o = S(i)$. The output is a set $o = \{o_1, o_2, \dots, o_m\}$ of signals (a.k.a. output signals), one per output. Figure 3b shows the output of the AT model corresponding to the input in figure 3a. The output is made by three output signals associated with the Speed, RPM, and Gear outputs.

Fitness Assessment (3). ATHeNA-S computes fitness measure $f(o)$ associated with the output of the system execution. Notice that since connections within the Simulink® model can directly connect inputs to outputs, fitness measures can also use information from inputs signals to guide the search. ATHeNA-S implements the ATHeNA framework by enabling the computation of the fitness measure as explained in steps [4] - [6].

AThENA *Fitness* (4). It is a function that combines the values computed by the manually defined and automatically generated fitness functions as follows:



(a) Example of input signals for the AT model.



(b) Output signals for the AT model for the input of figure 3a.

Figure 3: Example input and output for the AT Simulink® model.

$$f = f_a \cdot p + f_m \cdot (1 - p)$$

where p is a parameter within the range $[0, 1]$. ATheNA-S considers solely the value of the automatic fitness when $p = 1$, and solely the value of the manual fitness when $p = 0$. The higher the value of p , the more the automatic fitness value is prioritized. The lower the value of p , the more the manual fitness value is prioritized. For example, engineers may set the parameter p to the value 0.5 to equally prioritize manual and automatic fitness measures when analyzing the AT model.

Notice that ATheNA-S can use more complex functions to combine the manual and automatic fitness measures or it can dynamically change the fitness function during the search (e.g., [96]).

Automatic Fitness (5). ATheNA-S enables engineers to automatically generate fitness functions from a requirement φ expressed using a temporal logic-based formalism, such as Signal Temporal Logic (STL) [58] or Restricted Signals First-Order Logic (RFOL) [68]. For example, consider requirement AT1 that specifies that the value of the Speed output signal shall be lower than 120rpm for every instant within $[0, 20]$ time interval. The requirement can be expressed in STL as

$$\mathcal{G}_{[0,20]}(\text{Speed} < 120),$$

where “Speed<120” is a predicate indicating that the “Speed” is lower than the value “120”, \mathcal{G} is the “globally” temporal operator, and $[0, 20]$ is a time interval indicating that the predicate must hold from the time instant “0” to the time instant “20”. ATheNA-S automatically translates the STL specification into a fitness function f_a . The value generated by the fitness function f_a is negative if the property is violated and positive otherwise. In addition, the higher is the positive value computed by f_a , the farther the system from violating its requirement; and the lower is the negative value, the farther the system from satisfying its requirement.

Manual Fitness (6). ATheNA-S enables engineers to define a fitness function that considers the output (o) of the Simulink® simulation, the model of system S , and assumption A for the computation

of fitness value f_m . For example, the function below is a possible fitness function for the AT model, given a property that requires the vehicle speed to be lower than 120mph at all times.

$$f_m = \text{mean}(\text{Brake}) - \text{mean}(\text{Throttle}),$$

where $\text{mean}(\text{Throttle})$ and $\text{mean}(\text{Brake})$ are the average values assumed by the Throttle and Brake input signals over the simulation time. The value assumed by $\text{mean}(\text{Throttle})$ increases as the average value assumed by the input signal Throttle increases. The value assumed by $\text{mean}(\text{Brake})$ decreases as the average value assumed by the input signal Brake decreases. Since ATheNA minimizes the value computed by the fitness function, the function f_m guides the search toward areas of the input domain with high Throttle and low Brake values that are more likely to make the speed of the vehicle higher than 120mph. Specifically, the higher the value of the $\text{mean}(\text{Throttle})$, the lower the value computed by f_m , and the lower the value of the $\text{mean}(\text{Brake})$, the lower the value computed by f_m .

4 IMPLEMENTATION

We implement ATheNA-S as a plugin for S-Taliro [10], an open-source SBST tool. We selected S-Taliro, among other alternatives (e.g., BREACH [26], FaLCAuN [94], falsify [97], FaLSTAR [31, 93], FORESEE [98]) due to its recent classification as ready for industrial development [48], and its use in several industrial systems (e.g., [90]). In addition, this choice makes our solution applicable with other S-Taliro plugins, such as Aristeo [67].

ATheNA-S reuses the modules provided by S-Taliro to implement the input generation (1) and system execution (2) steps of ATheNA. For the input generation step, S-Taliro provides a set of alternatives that rely on different search algorithms, such as Simulated Annealing [2], Monte Carlo [70], and gradient descent methods [3]. For the system execution step, S-Taliro relies on the `sim` command of Matlab [85] to run the Simulink® simulator.

Listing 1: ATheNA-S Implementation.

```

1 classdef (Abstract) F_Assessment
2     methods (Abstract=true)
3         fa=autFitness(S,A,phi,i,o);
4         fm=manFitness(S,A,phi,i,o);
5         f=athenaFitness(S,A,phi,i,o);
6         s=stopCriterion(S,A,phi,i,o);
7     end
8 end
9
10 classdef AT1_F_Assessment < F_Assessment
11     methods
12         function fa=autFitness(S,A,phi,i,o)
13             return callTaliro(o,phi,[...]);
14         end
15         function fm=manFitness(S,A,phi,i,o)
16             throttlef=scale(mean(i(:,1)), A(1).R);
17             brakef=scale(mean(i(:,2)), A(2).R);
18             return brakef-throttlef;
19         end
20         function f=athenaFitness(S,A,phi,i,o)
21             return 0.5*autFitness(S,A,phi,i,o)
22                 +0.5*manFitness(S,A,phi,i,o);
23         end
24         function s=stopCriterion(S,A,phi,i,o)
25             return autFitness(S,A,phi,i,o) < 0;
26         end
27     end
28 end

```

ATheNA-S modifies the fitness assessment step of S-Taliro (3) as described in Section 3. Specifically, we modified the source code of S-Taliro to receive a subclass of the F_Assessment abstract class as input to compute the fitness measure. The abstract class F_Assessment detailed in Listing 1 (Lines 1-8) describes the generic common functionalities of ATheNA-S fitness functions. More precisely, it specifies that each ATheNA-S fitness measure has three methods: autFitness (Line 3), that specifies how the automatic fitness measure is computed (5), manFitness (Line 4), that specifies how the manual fitness measure is computed (6), and athenaFitness (Line 5), that specifies how the automatic and manual fitness values are combined (4). Finally, the stopCriterion method defines the condition that stops the search.

ATheNA-S allows for model-specific fitness functions that combine manually defined and automatically generated fitness functions. For example, the subclass AT1_F_Assessment, detailed in Listing 1 (Lines 10-28), provides the implementation for the methods of the class F_Assessment for the requirement AT1 of AT.

The method autFitness (Lines 12-14), that computes the value of the automated fitness function, is implemented by using the method callTaliro provided by S-Taliro. As done in the default implementation of S-Taliro, we provided the output signals (o) generated by running the Simulink® model as inputs to the method CallTaliro, together with the property phi, and some additional configuration parameters omitted for brevity ([...] in Line 13).

Method manFitness (Lines 15-19) implements the manual fitness function by defining variables throttlef (Line 16) and brakef (Line 17). The variable throttlef contains the average (mean(i(:,1))) of the values stored in the first column (i(:,1)) of the input (i), that is average of the values assumed by the Throttle input signal. This value is scaled (scale) within [0, 1], by considering the value range (A(1).R) for the throttle. The higher the values

associated with the Throttle, the higher is the value assumed by the variable throttlef. The variable brakef contains the average (mean(i(:,2))) of the values stored in the second column (i(:,2)) of the input (i), that is the average of the values assumed by the Brake input signal, scaled within the range [0, 1]. The manual fitness function value is the difference between the value of the variable brakef and the value of the variable throttlef (Line 18), which is within the range [-1, 1]. The value -1 means throttle is maximum and no brake is applied and the value 1 indicates the opposite. Notice that, since the goal of the search is to minimize the fitness value, our manual fitness function ensures that input signals with high Throttle and low Brake are prioritized during the search.

The athenaFitness method (Lines 20-23), that computes the value of the ATheNA fitness function, computes the sum of the product of the values assumed by the automated and the manual fitness functions and the value 0.5. Since the values of automated and manual fitness functions are within the range [-1, 1], this fitness function ensures that the ATheNA fitness value is also within the range [-1, 1] and both the manual and the automated fitness functions are equally prioritized.

The stopCriterion method (Lines 24-26), implementing the stopping criterion, aborts the search whenever the value computed by the automated fitness function is lower than 0. This stopping criterion reflects the robustness semantics of STL [36], i.e., a negative value indicates that the STL specification of the AT1 requirement is violated.

5 EVALUATION

In this section, we empirically evaluate ATheNA-S by considering the following research questions:

- RQ1 How *effective* is ATheNA-S in generating failure-revealing test cases? (Section 5.1)
- RQ2 How *efficient* is ATheNA-S in generating failure-revealing test cases? (Section 5.2)
- RQ3 How *applicable and useful* is ATheNA-S in generating failure-revealing test cases for a large automotive model? (Section 5.3)

To evaluate the effectiveness (RQ1) and efficiency (RQ2) of our solution, we compare ATheNA-S with existing SBST frameworks that only support either automatic or manual fitness functions. We consider S-Taliro as baseline framework supporting automatic fitness functions for the reasons explained in Section 4. We could not identify a SBST framework to be used as baseline for manual fitness functions since (a) SBST frameworks that rely on manual fitness functions are generally problem-specific, (b) we are not aware of a *generic* SBST framework based on manual fitness functions for Simulink® models. Thus, for manual fitness functions, we consider ATheNA-S and use an alternative implementation for the class F_Assessment (Listing 1) that forces the “athenaFitness” method (Line 5) to return the value computed by the manual fitness function, that is the value computed by the method “manFitness”. The implementation is obtained by considering the function *f* presented in Section 3 and by setting 0 as value for the parameter *p*. We refer to this instance of ATheNA as ATheNA-SM.

Table 1: Identifier (MID), description, number of blocks (#Blocks), inports (#Inport), outputs (#Output), simulation time in seconds (Ts), and requirements (#Reqs) of our benchmark models.

MID	Description	#Blocks	#Inport	#Output	Ts	#Reqs
AT	A model of a car automatic transmission with gears from 1 to 4.	69	2	3	50	10
AFC	A controller for the air-fuel ratio in an engine.	302	2	3	50	3
NN	A Neural Network controller for a levitating magnet above an electromagnet.	111	1	1	40	2
WT	A model of a wind turbine that takes as input the wind speed.	161	1	6	630	4
CC	A simulation of a system formed by five cars.	13	2	5	100	6
F16	Simulation of an F16 ground collision avoidance controller.	55	0	4	15	1
SC	Dynamic model of steam condenser, controlled by a Recurrent Neural Network.	172	1	4	35	1

Table 2: Identifier (RID), formal specification, and description for the requirements of the different models.

RID	STL Specification	Description
AT1	$\mathcal{G}_{[0,20]}(\text{Speed} < 120)$	The value of the speed within the interval $[0, 20]$ s shall be lower than 120mph.
AT2	$\mathcal{G}_{[0,10]}(\text{RPM} < 4750)$	The value of the motor speed within the interval $[0, 10]$ s shall be lower than 4750rpm.
AT51	$\mathcal{G}_{[0,30]}((\neg g1 \wedge \mathcal{F}_{[0.001,0.1]} g1) \Rightarrow \mathcal{F}_{[0.001,0.1]}(\mathcal{G}_{[0.2,5]} g1))$	If gear one is engaged at any time in $[0, 30]$ s, it shall remain engaged for at least 2.5s.
AT52	$\mathcal{G}_{[0,30]}((\neg g2 \wedge \mathcal{F}_{[0.001,0.1]} g2) \Rightarrow \mathcal{F}_{[0.001,0.1]}(\mathcal{G}_{[0.2,5]} g2))$	If gear two is engaged at any time in $[0, 30]$ s, it shall remain engaged for at least 2.5s.
AT53	$\mathcal{G}_{[0,30]}((\neg g3 \wedge \mathcal{F}_{[0.001,0.1]} g3) \Rightarrow \mathcal{F}_{[0.001,0.1]}(\mathcal{G}_{[0.2,5]} g3))$	If gear three is engaged at any time in $[0, 30]$ s, it shall remain engaged for at least 2.5s.
AT54	$\mathcal{G}_{[0,30]}((\neg g4 \wedge \mathcal{F}_{[0.001,0.1]} g4) \Rightarrow \mathcal{F}_{[0.001,0.1]}(\mathcal{G}_{[0.2,5]} g4))$	If gear four is engaged at any time in $[0, 30]$ s, it shall remain engaged for at least 2.5s.
AT6a	$(\mathcal{G}_{[0,30]}(\text{RPM} < 3000)) \Rightarrow (\mathcal{G}_{[0,4]}(\text{Speed} < 35))$	If RPM is lower than 3000 within $[0, 30]$ s, then Speed shall be lower than 35 in the interval $[0, 4]$ s.
AT6b	$(\mathcal{G}_{[0,30]}(\text{RPM} < 3000)) \Rightarrow (\mathcal{G}_{[0,8]}(\text{Speed} < 50))$	If RPM is lower than 3000 within $[0, 30]$ s, then Speed shall be lower than 50 in the interval $[0, 8]$ s.
AT6c	$(\mathcal{G}_{[0,30]}(\text{RPM} < 3000)) \Rightarrow (\mathcal{G}_{[0,20]}(\text{Speed} < 65))$	If RPM is lower than 3000 within $[0, 30]$ s, then Speed shall be lower than 65 in the interval $[0, 20]$ s.
AT6abc	$\text{AT6a} \wedge \text{AT6b} \wedge \text{AT6c}$	The requirements with RID AT6a, AT6b, AT6c shall be satisfied.
AFC27	$\mathcal{G}_{[11,50]}((\text{rise} \vee \text{fall}) \rightarrow (\mathcal{G}_{[1,5]} \mu < 0.008))$	If within $[11, 50]$ s the throttle angle rises or falls, then the error (μ) shall be lower than 0.008.*
AFC29	$\mathcal{G}_{[11,50]}(\mu < 0.007)$	Within $[11, 50]$ s, the error shall be lower than 0.007.†
AFC33	$\mathcal{G}_{[11,50]}(\mu < 0.007)$	Within $[11, 50]$ s, the error shall be lower than 0.007.§
NN	$\mathcal{G}_{[1,37]}((Pos - Ref > (0.005 + 0.03 Ref)) \rightarrow \mathcal{F}_{[0,2]} \mathcal{G}_{[0,1]} \neg(0.005 + 0.03 Ref \leq Pos - Ref))$	The discontinuities between the levitating magnet position (<i>Pos</i>) and the reference position (<i>Ref</i>) shall be at least 3 time units apart.
NNx	$\mathcal{G}_{[0,1]}(Pos > 3.2) \wedge \mathcal{F}_{[1,1.5]}(\mathcal{G}_{[0,0.5]}(1.75 < Pos < 2.25)) \wedge \mathcal{G}_{[2,3]}(1.825 < Pos < 2.175)$	The magnet position (<i>Pos</i>) shall be higher than 3.2 within $[0, 1]$ s, lower than 2.175 and higher than 1.825 within $[2, 3]$ s, and higher than 1.75 and lower than 2.25 for 0.5s within $[2, 3]$ s.
WT1	$\mathcal{G}_{[30,630]}(\theta \leq 14.2)$	The pitch angle shall be smaller than 14.2deg.
WT2	$\mathcal{G}_{[30,630]}(21000 \leq M_{g,d} \leq 47500)$	The torque shall be between 21000 and 47500N·m.
WT3	$\mathcal{G}_{[30,630]}(\Omega \leq 14.3)$	The rotor speed shall be lower than 14.3rpm.
WT4	$\mathcal{G}_{[30,630]} \mathcal{F}_{[0,5]}(\theta - \theta_d \leq 1.6)$	The absolute difference between the commanded and the measured pitch angles is lower than 1.6deg.
CC1	$\mathcal{G}_{[0,100]}(y_5 - y_4 \leq 40)$	Within the interval $[0, 100]$ s, the difference between y_5 and y_4 shall be lower than 40.
CC2	$\mathcal{G}_{[0,70]} \mathcal{G}_{[0,30]}(y_5 - y_4 \geq 15)$	For every instant in $[0, 70]$ s, the value of $y_5 - y_4$ shall exceed 15 in one instant within the next 30s.
CC3	$\mathcal{G}_{[0,80]}((\mathcal{G}_{[0,20]}(y_2 - y_1 \leq 20)) \vee (\mathcal{F}_{[0,20]}(y_5 - y_4 \geq 40)))$	For every instant in $[0, 70]$ s, either $y_2 - y_1$ shall be lower than 20 for the next 20s or the value of $y_5 - y_4$ shall be higher than 40 for the next 20s.
CC4	$\mathcal{G}_{[0,65]} \mathcal{F}_{[0,30]} \mathcal{G}_{[0,20]}(y_5 - y_4 \geq 8)$	For every instant in $[0, 65]$ s, within the next 30s, $y_5 - y_4$ shall be higher than 8 for at least 20s.
CC5	$\mathcal{G}_{[0,72]} \mathcal{F}_{[0,8]}((\mathcal{G}_{[0,5]}(y_2 - y_1 \geq 9)) \rightarrow (\mathcal{G}_{[5,20]}(y_5 - y_4 \geq 9)))$	For every time instant in $[0, 72]$ s, if within the next 8s the value of $y_2 - y_1$ is higher than 9 for at least 5s, after 5s the value of $y_5 - y_4$ shall be higher than 9 and remain higher than 9 for the following 15s.
CCx	$\bigwedge_{i=1..4} \mathcal{G}_{[0,50]}(y_{i+1} - y_i > 7.5)$	Within the interval $[0, 50]$ s, the difference between y_{i+1} and y_i shall be higher than 7.5.
F16	$\mathcal{G}_{[0,15]}(\text{altitude} > 0)$	Within the interval $[0, 15]$ s, the altitude shall be higher than 0.
SC	$\mathcal{G}_{[30,35]}(87 \leq \text{pressure} \leq 87.5)$	Within the interval $[30, 35]$ s, the pressure shall be lower than 87.5 and higher than 87.

* $\text{rise} = (\theta < 8.8) \wedge (\mathcal{F}_{[0,0.005]}(\theta > 40.0))$, $\text{fall} = (\theta > 40.0) \wedge (\mathcal{F}_{[0,0.005]}(\theta < 8.8))$, $0 \leq \theta < 61.2$

† The range of the throttle angle is $0 \leq \theta < 61.2$.

§ The range of the throttle angle is $61.2 \leq \theta \leq 81.2$.

To evaluate the effectiveness of the tools, we considered a benchmark made by seven models and 27 requirements. We evaluate the capability of each tool in generating failure-revealing test cases. To assess the efficiency of the tools, we compare the number of search iterations (see figure 1) required by each tool to generate the failure-revealing test cases.

To assess the applicability (RQ3) of ATheNA-S, we evaluate its effectiveness and efficiency in a large and representative case study from the automotive domain. We inject a fault in the model by relying on the insights of a lead engineer in a large automotive company and evaluate whether ATheNA-S could generate a failure-revealing test case.

Implementation and Data Availability. Our (sanitized) models, data, and tool are publicly available [17].

5.1 Effectiveness – RQ1

We compare the effectiveness of S-Taliro, ATheNA-SM and ATheNA-S in generating failure-revealing test cases.

Benchmark. We consider the models of the ARCH competition [33] – an international competition among testing tools for continuous and hybrid systems [11]. This benchmark consists of seven models: Automatic Transmission (AT), Fuel Control on Automotive Powertrain (AFC), Neural Network Controller (NN), Wind

Table 3: Interpolation function (int), value range (R and R'), and number of control points (n) for the input signals.

RID	int	R	R'	n	RID	int	R	R'	n
AT1	pchip,pchip	[0, 100], [0, 325]	[0, 110], [0, 100]	7, 3	NNx	pchip	[1.95, 2.05]	[1.95, 2.14]	3
AT2	pchip,pchip	[0, 100], [0, 325]	[0, 90], [32, 325]	7, 3	WT1	pchip	[8, 16]	[7.5, 16.5]	126
AT51	pchip,pchip	[0, 100], [0, 325]		7, 3	WT2	pchip	[8, 16]		126
AT52	pchip,pchip	[0, 100], [0, 325]		7, 3	WT3	pchip	[8, 16]		126
AT53	pchip,pchip	[0, 100], [0, 325]		7, 3	WT4	pchip	[8, 16]		126
AT54	pchip,pchip	[0, 100], [0, 325]		7, 3	CC1	pchip,pchip	[0, 1], [0, 1]	[0, 0.82], [0.18, 1]	7, 3
AT6a	pchip,pchip	[0, 100], [0, 325]	[0, 47], [172, 325]	7, 3	CC2	pchip,pchip	[0, 1], [0, 1]		7, 3
AT6b	pchip,pchip	[0, 100], [0, 325]	[0, 48], [169, 325]	7, 3	CC3	pchip,pchip	[0, 1], [0, 1]		7, 3
AT6c	pchip,pchip	[0, 100], [0, 325]	[0, 44], [182, 325]	7, 3	CC4	pchip,pchip	[0, 1], [0, 1]		7, 3
AT6abc	pchip,pchip	[0, 100], [0, 325]	[0, 44], [182, 325]	7, 3	CC5	pchip,pchip	[0, 1], [0, 1]		7, 3
AFC27	const,pconst	[900, 1100], [0, 61.2]		1, 10	CCx	pchip,pchip	[0, 1], [0, 1]		7, 3
AFC29	const,pconst	[900, 1100], [0, 61.2]		1, 10	F16	const,const	[0.63, 0.89], [-1.26, -1.10],	[0.16, 0.89], [-1.26, -0.63],	1, 1
AFC33	const,pconst	[900, 1100], [61.2, 81.2]		1, 10	const		[-1.18, -0.39]	[-1.83, -0.39]	1
NN	pchip	[1, 3]	[1, 2]	3	SC	pchip,pchip	[3.99, 4.01]	[3.984, 4.016]	20

pchip: piecewise cubic, const: constant signal, pconst: piecewise constant signal.

Table 4: Manual fitness functions description for our benchmark requirements.

RID	Manual Fitness Description
AT1	Maximizes the lowest throttle value within [0, 17]s and minimizes the highest brake value within [0, 25]s.
AT2	Maximizes the average throttle value within [0, 8]s, then minimizes the average brake value within [0, 25]s.
AT51	Maximizes the lowest throttle value within [0, 33]s and minimizes the highest brake value within [0, 25]s.
AT52	Maximizes the lowest throttle value within [0, 33]s and minimizes the highest brake value within [0, 25]s.
AT53	Maximizes the lowest throttle value within [0, 33]s and minimizes the highest brake value within [0, 25]s.
AT54	Maximizes the lowest throttle value within [0, 33]s and minimizes the highest brake value within [0, 25]s.
AT6a	Makes the average throttle value within [0, 33]s as close as possible to 45% and minimizes the average brake value within [0, 25]s.
AT6b	Makes the average throttle value within [0, 33]s as close as possible to 45% and minimizes the average brake value within [0, 25]s.
AT6c	Makes the average throttle value within [0, 33]s as close as possible to 45% and minimizes the average brake value within [0, 25]s.
AT6abc	Makes the average throttle value within [0, 33]s as close as possible to 45% and minimizes the average brake value within [0, 25]s.
AFC27	Increases the two control points adjacent to the lowest one until they are both above 40 deg, then minimizes the lowest value within [10, 50]s.
AFC29	Minimizes the lowest throttle value within [10, 50]s.
AFC33	Minimizes the engine speed value.
NN	Minimizes the reference position control point at 20s.
NNx	Maximizes the lowest reference position within [0, 20]s.
WT1	Maximizes the steepest positive slope between two consecutive control points within [30, 630]s.
WT2	Maximizes the steepest negative slope between two consecutive control points within [30, 630]s.
WT3	Maximizes the steepest positive slope between two consecutive control points within [30, 630]s.
WT4	Maximizes the average distance between consecutive control points within [30, 630]s.
CC1	Maximizes the lowest throttle value within [0, 100]s and minimizes the highest brake value within [0, 100]s.
CC2	Minimizes the highest throttle value within [0, 100]s and maximizes the lowest brake value within [0, 100]s.
CC3	Maximizes the lowest throttle value within [0, 100]s and minimizes the highest brake value within [0, 100]s.
CC4	Minimizes the minimum distance between car 4 and 5 within [0, 100]s.
CC5	Makes the average throttle value within [0, 33]s as close as possible to 0.3 and maximizes the average brake value within [0, 50]s.
CCx	Maximizes the throttle control point at 0s and minimizes the throttle control point at 17s.
F16	Maximizes the initial roll angle and minimizes the initial pitch angle.
SC	Maximizes the peak-to-peak distance of the steam flow rate within [29.5, 35]s.

Turbine (WT), Chasing Cars (CC), Aircraft Ground Collision Avoidance System (F16), and Steam Condenser (SC). For each model, Table 1 contains a model identifier (MID), a short description of the model, the number of Simulink® blocks (#Blocks), inputs (#Inport), outputs (#Outport), simulation time (Ts), and number of requirements (#Reqs). The number of blocks, inputs, and outputs respectively varies across the different models.

The models of the ARCH competition are associated with the 27 requirements presented in Table 2. Table 2 presents the STL specification and a short description for each requirement. Requirements are associated with a requirement identifier (RID) that starts with the identifier of the model. For example, the requirement with identifier AT54 refers to the AT model. The symbols “ \mathcal{G} ” and “ \mathcal{F} ” used in the STL specification represent the “globally” and “eventually”

temporal operators. The “globally” temporal operator is discussed in Section 3. The “eventually” temporal operator is labeled with a subscript containing the time interval to consider when assessing the operator. For example, “ $\mathcal{F}_{[0,10]}$ ” indicates that the “eventually” temporal operator must be assessed over the time interval [0, 10]s. The operator scopes a condition that shall eventually hold within the time interval. For example, “ $\mathcal{F}_{[0,10]} x < 5$ ” indicates that the value of x shall be lower than 5 at some point within the interval [0, 10]s. The requirements of our benchmark have a different structure and use various temporal operators.

For each requirement, Table 3 presents the assumptions considered in the ARCH competition that we use for generating the test cases. Specifically, for each requirement of our benchmark, the table reports the interpolation function (int), value range (R and R'),

Table 5: Percentage of failure-revealing runs for each of the tool and assumption-requirement combination of Table 3.

RID	S-Taliro	ATheNA-SM	ATheNA-S	RID	S-Taliro	ATheNA-SM	ATheNA-S	RID	S-Taliro	ATheNA-SM	ATheNA-S
AT1	0 % (18 %)	2 % (78 %)	2 % (78 %)	AT6abc	96 % (6 %)	46 % (32 %)	98 % (18 %)	WT4	50 %	42 %	58 %
AT2	100 % (92 %)	100 % (88 %)	100 % (92 %)	AFC27	38 %	52 %	48 %	CC1	100 % (100 %)	98 % (96 %)	100 % (100 %)
AT51	100 %	100 %	100 %	AFC29	100 %	100 %	100 %	CC2	84 %	92 %	96 %
AT52	100 %	100 %	100 %	AFC33	0 %	0 %	0 %	CC3	92 %	88 %	94 %
AT53	100 %	100 %	100 %	NN	74 % (78 %)	68 % (86 %)	68 % (82 %)	CC4	0 %	0 %	6 %
AT54	100 %	100 %	100 %	NNx	0 % (90 %)	0 % (100 %)	0 % (100 %)	CC5	84 %	98 %	98 %
AT6a	100 % (58 %)	40 % (36 %)	96 % (86 %)	WT1	2 % (94 %)	2 % (94 %)	4 % (96 %)	CCX	62 %	42 %	80 %
AT6b	88 % (38 %)	34 % (32 %)	92 % (56 %)	WT2	92 %	92 %	92 %	F16	76 % (90 %)	100 % (98 %)	100 % (96 %)
AT6c	90 % (6 %)	54 % (32 %)	90 % (18 %)	WT3	92 %	82 %	90 %	SC	0 % (34 %)	0 % (30 %)	0 % (34 %)

and the number of control points (n) considered for generating the test input signals. Comma-separated values are related to different input signals. For example, for AT1, $[0, 100]$ and $[0, 325]$ are respectively the value ranges considered for generating the Throttle and the Brake input signals. Notice that while the configuration of the ARCH competition includes the input ranges, it does not include the number of control points and the interpolation functions as different SBST frameworks can use different strategies to generate the input signals. Thus, we select the setting used by Aristeo in the last competition since the complete replication package is publicly available [13]. For some of the requirements for which the tools are showing a similar behavior considering the value range R of the ARCH 2021 competition (see the **Results** paragraph), we consider an additional value range R' that enables a wider comparison between the tools.

In total, Table 3 leads to 39 assumption-requirement combinations. Each combination consists of a requirement and an assumption generated by considering the interpolation function, the number of control points, and one of the value ranges specified for that requirement. For example, two combinations are present for requirement AT1, generated by considering value ranges R and R' . In our evaluation, we compare the behavior of the different tools by considering each assumption-requirement combination.

Configuration of the Tools. We configure our tools as follows. For S-Taliro, we use its Simulated Annealing, its default search algorithm. We set the value 300 for the maximum number of iterations since this is the value considered by the ARCH competition.

We configure ATheNA-SM by designing a manual fitness function for each requirement by reverse-engineering the model and performing some trial error experiments. Table 4 presents the manual fitness functions defined for each requirement. For example, for the AT1 requirement, we design a fitness function that maximizes the value of Throttle and minimizes the value of Brake (Section 3). Since ATheNA-SM relies on S-Taliro, we considered the same configuration as S-Taliro for the common parameters.

We configure ATheNA-S by considering the implementation of the method *athenaFitness* that equally prioritizes the manual and the automated fitness functions (Listing 1). For the other parameters we considered the same configuration of ATheNA-SM.

Methodology. We execute S-Taliro, ATheNA-SM, and ATheNA-S for each of the 39 assumption-requirement combinations of Table 3. For each combination, we run each experiment 50 times to consider the stochastic nature of the algorithm, as done in similar works (e.g., [67]) and mandated by the ARCH competition [33]. We run our experiments on a large computing platform and, for each tool,

we record which of the 50 runs is a *failure-revealing run*, i.e., it returns a failure-revealing test case.

Results. Running all the experiments required approximately 35 days. We reduced the time to seven days by exploiting the parallelization facilities of our computing platform.¹

For each tool and assumption-requirement combination, Table 5 presents the percentage of failure-revealing runs (over 50 runs). The table reports the results obtained by considering the assumption-requirement combination obtained by considering the value range R , and the one obtained by considering the value range R' (within round brackets). For example, for the AT1 requirement, S-Taliro returned a failure-revealing test case for 0% and 18% of the runs for the assumptions obtained from the value ranges R and R' .

For $\approx 79\%$ of the combinations (31 out of 39), represented using non-bold characters in Table 5, the percentage of failure-revealing runs of ATheNA-S is higher than or equal to the one of S-Taliro and ATheNA-SM. For these combinations, ATheNA-S has to be preferred since, in the worst-case, it works as the best among S-Taliro and ATheNA-SM. The increment ATheNA-S provides on the percentage of failure-revealing runs is on average 6.8% ($min=0\%$, $max=60\%$, $StdDev=12.6\%$) when ATheNA-S is compared with S-Taliro, and it is 9.9% ($min=0\%$, $max=58\%$, $StdDev=17.5\%$) when ATheNA-S is compared with ATheNA-SM.

Remarkably, unlike S-Taliro and ATheNA-SM, ATheNA-S generated failure-revealing test cases for CC4, i.e., ATheNA-S detected failures other tools could not find.

For only $\approx 21\%$ of the assumption-requirement combinations (8 out of 39), represented using bold characters in Table 5, ATheNA-S generated less failure-revealing runs than (at least one of) the baselines. For these cases, the penalty of ATheNA-S is negligible: the percentage of failure-revealing runs is only 4% (for AT6a), 14% (for AT6c), 14% (for AT6abc), 4% (for AFC27), 6% and 4% (for NN), 2% (for WT3), 2% (for F16) lower than the best baseline framework. The decrement of ATheNA-S in the percentage of failure-revealing runs is on average 4.0% ($min=2\%$, $max=6\%$, $StdDev=2.0\%$) when it is compared with S-Taliro and 7.6% ($min=2\%$, $max=14\%$, $StdDev=5.9\%$) when it is compared with ATheNA-SM.

Considering all the 39 assumption-requirement combinations, the percentage of failure-revealing runs of ATheNA-S is on average 6.3% ($min=-6\%$, $max=60\%$, $StdDev=11.6\%$) and 8.6% ($min=-14\%$, $max=58\%$, $StdDev=18.5\%$) higher than S-Taliro and ATheNA-SM.

¹ 1109 nodes, 64 cores, memory 249G or 2057500M, CPU 2 x AMD Rome 7532 2.40 GHz 256M cache L3.

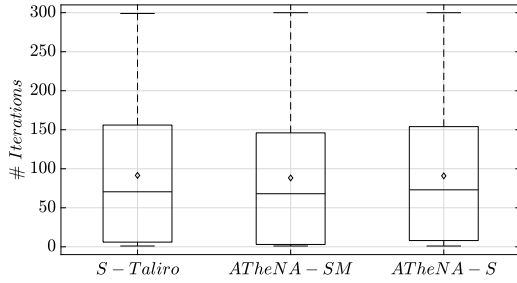


Figure 4: Number of iterations of S-Taliro, ATheNA-SM, and ATheNA. Diamonds depict the average.

The Wilcoxon rank sum test [65] confirms that ATheNA-S generates more failure-revealing runs than S-Taliro and ATheNA-SM with level of significance 0.174.

RQ1 - Effectiveness

The answer to RQ1 is that, ATheNA-S is preferable over the baseline tools for $\approx 79\%$ of our assumption-requirement combinations. ATheNA-S generated on average 6.3% ($min=-6\%$, $max=60\%$, $StdDev=11.6\%$) and 8.6% ($min=-14\%$, $max=58\%$, $StdDev=18.5\%$) more failure-revealing runs than S-Taliro and ATheNA-SM. For one combination, unlike S-Taliro and ATheNA-SM, ATheNA-S generated failure-revealing test cases.

5.2 Efficiency – RQ2

To compare the efficiency of S-Taliro, ATheNA-SM, and ATheNA-S in generating failure-revealing test cases, we proceed as follows.

Methodology. We analyze the results of the experiment conducted for answering RQ1. Since for each iteration, the difference in the execution time of S-Taliro, ATheNA-SM, and ATheNA-S is negligible, we use the number of iterations as the metric to compare the efficiency of the considered tools. For each tool, we consider the failure-revealing runs from RQ1 and extract the number of iterations required to generate the failure-revealing test cases.

Results. The box plots in figure 4 report the number of iterations S-Taliro, ATheNA-SM, and ATheNA-S require to generate the failure-revealing test cases. Our results show that ATheNA-S requires on average more iterations than S-Taliro ($avg=6.9$, $min=-61.5$, $max=72.2$, $StdDev=24.8$) and less iterations than ATheNA-SM ($avg=-1.6$, $min=-116.5$, $max=42.0$, $StdDev=27.1$). However, the overhead ATheNA-S brings about over S-Taliro tools is negligible: the time required by ATheNA-S to perform one iteration for the WT model, the model that requires the highest time to perform an iteration, is 3s. Therefore, for the model with the highest simulation time, the average overhead introduced by ATheNA-S is only 21s ($3s \times 6.9iterations$). This is acceptable for practical applications since the maximum overhead (less than 1m) is significantly lower than the time required to develop the models, typically months for large industrial models [21].

The Wilcoxon rank sum test [65] confirms that, for the tools we compared, there is no statistical difference between the number of iterations required to generate failure-revealing test cases ($p=0.05$).

RQ2 - Efficiency

The answer to RQ2 is that, for our assumption-requirement combinations, ATheNA-S requires slightly more iterations than S-Taliro ($avg=6.9$, $min=-61.5$, $max=72.2$, $StdDev=24.8$), and slightly less than ATheNA-SM ($avg=-1.6$, $min=-116.5$, $max=42.0$, $StdDev=27.1$) to generate failure-revealing test cases.

5.3 Usefulness – RQ3

To assess the usefulness of ATheNA-S, we evaluate its applicability to a large automotive case study.

Case Study. Our case study is the Simulink® model of a hybrid-electric vehicle (HEV) developed for the EcoCAR Mobility Challenge [30], a competition sponsored by the U.S. Department of Energy [25], General Motors [39], and MathWorks [60]. The HEV motor converts electrical energy into mechanical energy. A software controller regulates the behavior of the motor.

The HEV model includes multiple subsystems built using Add-Ons components of Simulink®, including Simscape [83], Simscape Electrical [84], and Simscape Driveline [28]. The controller is modeled with Simulink® Stateflow [86]. The controller input is the speed demand, i.e., the required speed in Kph (kilometer per hour), and its output is the vehicle speed. The HEV model contains three input exemplars with the speed demand for three urban driving scenarios.

Methodology. To generate realistic driving scenarios, we consider one of the three urban driving scenarios exemplars and slightly vary the speed demand. Specifically, we add the input signal `delta_i_speed` to the HEV model that represents the variation applied to the speed demand of the urban driving scenario we considered. We set the value 400s for the simulation time, since it is the simulation time provided for the HEV model.

To use ATheNA-S, we first need to design assumptions for the `delta_i_speed` input signal. We set $[0, 4]$ Kph as the value range for the assumption since it is a sufficiently small range for the variation of the speed demand. We consider five control points to ensure speed variations occurring every 100s. We set the `pchip` interpolation function [74] since it generates smooth and continuous signals for the variations of the speed demand.

The requirement we consider specifies that the difference between the desired speed and the vehicle speed after 0.7s shall be lower than a threshold value. We express the requirement in STL as

$$\mathcal{G}_{[0,400]}(\text{delta}_o_speed < \text{threshold}),$$

The variable `delta_o_speed` represents an output signal computing the difference between the vehicle speed and the desired demand 0.7s before. The temporal operator $\mathcal{G}_{[0,400]}$ requires the value of `delta_o_speed` to be lower than the threshold value within the interval $[0, 400]$ s. We set 3Kph for the threshold value since, for the urban driving scenario we considered, `delta_o_speed` was always lower than this value.

To prioritize inputs that generate significant changes for the speed demand, we define a manual fitness function that minimizes and maximizes the values of two consecutive control points of the input signal `delta_i_speed`. We use the implementation for the method `athenaFitness` from Listing 1 since it equally prioritizes the manual and the automated fitness functions.

We set the value 300 for the number of iterations. Then, we run ATheNA-S once. As expected, ATheNA-S could not generate any failure-revealing test case.

We use the insights of a lead engineer from a large automotive company to inject a representative fault in the model: we change the threshold that makes the car switch from the Cruise_mode to the Accelerate_mode by 50%.

We run ATheNA-S and check whether it could generate failure-revealing test cases for the faulty model.

Results. ATheNA-S generated a failure-revealing test in 12 iterations requiring 199s (≈ 3 min).

RQ3 - Usefulness

The answer to RQ3 is that, ATheNA-S was able to compute a failure-revealing test case for a large automotive case study.

6 DISCUSSION AND THREATS TO VALIDITY

For the benchmark models and requirements we consider, our results show that ATheNA-S is more effective in detecting failure-revealing test cases than the baseline frameworks with no significant performance overhead. Additionally, ATheNA-S was able to generate a failure-revealing test case for CC4 the baselines could not find. Finally, ATheNA-S was able to generate a failure-revealing test case for our case study. Based on these results, we recommend the following workflow. Engineers should initially use SBST frameworks based on automated fitness functions since they do not require manual effort to define the fitness functions and may already return failure-revealing test cases. If no failure-revealing test case is detected, engineers should use SBST frameworks based on manually defined fitness functions since they guide the search toward portions of the input domain that are more likely to contain failures. Finally, engineers should use SBST frameworks that combine automatically generated and manually defined fitness functions and can detect failures other frameworks can not find.

External Validity. The selection of the models and requirements is a threat to the external validity of our results. However, the benchmark models considered in RQ1 and RQ2 (a) were extensively used in the SBST literature (e.g., [27, 33, 34, 37, 47, 67]), (b) are representative from different CPS systems, i.e., AT, AFC, CC are from the automotive domain, NN is from the ML domain, WT is from the electrical domain, F16 is from the aerospace domain, (c) some of the models were developed by engineers working in the industry, i.e., AFC is from Toyota [47]. The case study used to answer RQ3 is a large and complex case study representative of industrial systems developed by MathWorks [60] and linked to the EcoCAR Mobility Challenge [30], a competition sponsored by the U.S. Department of Energy [25], General Motors [39].

The reverse-engineering process we used to define the manual fitness functions for ATheNA-SM (see Section 5.1), the fitness function of ATheNA-S, and the fault we injected are a threat to the external validity of our results. However, the results of ATheNA-SM and ATheNA-S are likely to improve when the designers of the fitness functions are knowledgeable about the domain and engineered the Simulink® models. For the fault definition, we use the insights of a lead engineer in a large automotive company.

ATheNA-S explicitly targets Simulink® models. Other instances of ATheNA can target different model types or software programs. We conjecture that our results are also generalizable to these domains. More empirical studies, such as that presented in this paper, will determine whether our conjecture holds.

Internal Validity. The values assigned to the configuration parameters of our tools are a threat to the internal validity of our results. However, our configuration does not favor any of the frameworks as the common configuration parameters of S-Taliro, ATheNA-SM, and ATheNA share the same values.

7 RELATED WORK

Despite the vast research literature on SBST and the considerable number of surveys on the topic (e.g., [6, 22, 43, 50, 53, 69]), we did not find any existing work classifying fitness functions into automatically generated and manually defined. In addition, we are not aware of any work proposing a framework that combines these two types of fitness functions. Therefore, this section summarizes related work targeting either *automatically generated* or *manually defined* fitness functions.

Automated generation of fitness function techniques often compute fitness functions from logic-based specifications (e.g., [27, 35, 36, 68, 73]). Well established SBST tools, such as BREACH [26], S-Taliro [10], Aristeo [67], and FALSTAR [93], rely on these fitness functions. For each atomic proposition, these fitness functions typically compute a value indicating a satisfaction degree for the proposition at every time instant. There are alternative ways to compute fitness values associated with temporal operators, such as the use of min and max operators [35, 36], distance operators computing smooth approximations of the min and max operators (e.g., [73]), arithmetic and geometric mean along a time interval (e.g., [56, 66, 92]), cumulative values over a time horizon (e.g., [41]). Some approaches also consider perturbations that may shift the signal values over time to compute the fitness value (e.g., [27]).

A variety of *manually defined* fitness functions was proposed in the literature. Manually defined fitness functions can guide the search to produce test outputs with diverse shapes [63], maximize or minimize the outputs of a system characterizing its critical behavior [20], maximize diversity in output signals [64], quantify the difference between a reference and an output signal [15], and minimize the difference between the expected and simulated behaviour of a CPS [46]. Many manually defined fitness functions were also proposed to guide SBST frameworks that analyze software code. For example, some recent manually defined fitness functions measure line coverage, input coverage, output coverage (e.g., [49]), branch distances (e.g., [72]), test length, method sequence diversity, and crash distance [24], the cumulative number of defects and the total amount of code to inspect [71]. Manually defined fitness functions can also compute exploration measures [61], and combine of coverage based and feature interaction measures [4].

Differently from these works, we proposed a framework that combines automatically generated and manually defined fitness functions and showed the benefits of our framework by considering a large benchmark made by seven models and 27 requirements and one complex case study from the automotive domain.

8 CONCLUSION

We presented ATheNA, a novel SBST framework that combines automatically generated and manually defined fitness functions. We defined ATheNA-S, an instance of ATheNA that supports Simulink® models. We assessed the benefits of ATheNA-S in generating failure-revealing test cases. ATheNA-S is preferable over the baseline tools for $\approx 79\%$ of our assumption-requirement combinations we considered in our evaluation. ATheNA-S generated more failure-revealing test cases than two baseline SBST frameworks that rely on automatically generated (+6.3%) and manually defined (+8.6%) fitness functions. ATheNA-S did not show statistically significant differences in efficiency compared with the baseline tools. Finally, ATheNA-S generated a failure-revealing test case for a large representative automotive case study. We discussed the impacts of our results on software engineering practices, and we suggested a workflow that combines ATheNA and SBST frameworks driven by automatically generated and manually defined fitness functions.

ACKNOWLEDGMENTS

We acknowledge the support of the Natural Sciences and Engineering Research Council of Canada (NSERC), [funding reference number RGPIN-2022-04622].

This research was enabled in part by support provided by Compute Ontario (www.computeontario.ca) and Compute Canada (www.computeCanada.ca).

REFERENCES

- [1] 2021. *Computer Safety, Reliability, and Security (SAFECOMP)*. Springer. <https://doi.org/10.1007/978-3-030-83903-1>
- [2] Houssam Abbas, Bardh Hoxha, Georgios Fainekos, and Koichi Ueda. 2014. Robustness-guided temporal logic testing and verification for stochastic cyber-physical systems. In *International Conference on Cyber Technology in Automation, Control and Intelligent*. IEEE, 1–6.
- [3] Houssam Abbas, Andrew Winn, Georgios Fainekos, and A Agung Julius. 2014. Functional gradient descent method for metric temporal logic specifications. In *American Control Conference*. IEEE, 2312–2317.
- [4] Raja Ben Abdesslem, Annibale Panichella, Shiva Nejati, Lionel C Briand, and Thomas Stifter. 2018. Testing autonomous cars for feature interaction failures using many-objective search. In *International Conference on Automated Software Engineering*. IEEE, 143–154.
- [5] Aldeida Aleti, Irene Moser, and Lars Grunske. 2017. Analysing the fitness landscape of search-based software testing problems. *Automated Software Engineering* 24, 3 (2017), 603–621. <https://doi.org/10.1007/s10515-016-0197-7>
- [6] Shaikat Ali, Lionel C. Briand, Hadi Hemmati, and Rajwinder Kaur Panesar-Walawege. 2010. A Systematic Review of the Application and Empirical Investigation of Search-Based Test Case Generation. *IEEE Transactions on Software Engineering* 36, 6 (2010), 742–762. <https://doi.org/10.1109/TSE.2009.52>
- [7] Hussein Almulla and Gregory Gay. 2020. Learning How to Search: Generating Exception-Triggering Tests Through Adaptive Fitness Function Selection. In *International Conference on Software Testing, Validation and Verification*. IEEE, 63–73.
- [8] Harald Altinger, Franz Wotawa, and Markus Schurius. 2014. Testing Methods Used in the Automotive Industry: Results from a Survey. In *Joining AcadeMiA and Industry Contributions to Test Automation and Model-Based Testing*. ACM, 1–6.
- [9] Boukhdhir Amal, Marouane Kessentini, Slim Bechikh, Josselin Dea, and Lamjed Ben Said. 2014. On the Use of Machine Learning and Search-Based Software Engineering for Ill-Defined Fitness Function: A Case Study on Software Refactoring. In *International Symposium on Search-Based Software Engineering*. Springer, 31–45.
- [10] Yashwanth Annpureddy, Che Liu, Georgios Fainekos, and Sriram Sankaranarayanan. 2011. S-TaLiRo: A Tool for Temporal Logic Falsification for Hybrid Systems. In *Tools and Algorithms for the Construction and Analysis of Systems*. Springer, 254–257.
- [11] ARCH 2022 [Online]. International Competition on Verifying Continuous and Hybrid Systems. <https://cps-vo.org/group/ARCH/FriendlyCompetition>
- [12] Andrea Arcuri and Lionel Briand. 2011. A practical guide for using statistical tests to assess randomized algorithms in software engineering. In *International Conference on Software Engineering*. ACM, 1–10.
- [13] ARISTEOWeb 2022 [Online]. ARISTEO – AppRoXimation-based TEst generatiOn. <https://github.com/SNTSVV/ARISTEO>.
- [14] Aitor Arrieta, Joseba A. Agirre, and Goiriura Sagardui. 2020. A Tool for the Automatic Generation of Test Cases and Oracles for Simulation Models Based on Functional Requirements. In *International Conference on Software Testing, Verification and Validation Workshops*. ACM/IEEE, 1–5.
- [15] Aitor Arrieta, Jon Ayerdi, Miren Illarramendi, Aitor Agirre, Goiriura Sagardui, and Maite Arratibel. 2021. Using Machine Learning to Build Test Oracles: an Industrial Case Study on Elevators Dispatching Algorithms. In *International Conference on Automation of Software Test*. IEEE, 30–39.
- [16] ATBenchmark 2022 [Online]. Modeling an Automatic Transmission Controller. <https://www.mathworks.com/help/simulink/slref/modeling-an-automatic-transmission-controller.html>.
- [17] ATheNA 2022 [Online]. ATheNA. <https://github.com/ATheNA-SBST/ATheNA>.
- [18] AUT 2022 [Online]. Automotive Electrical System Simulation and Control. <https://it.mathworks.com/matlabcentral/fileexchange/25674-automotive-electrical-system-simulation-and-control>.
- [19] Anu Bajaj and Om Prakash Sangwan. 2019. A Systematic Literature Review of Test Case Prioritization Using Genetic Algorithms. *IEEE Access* 7 (2019), 126355–126375. <https://doi.org/10.1109/ACCESS.2019.2938260>
- [20] Raja Ben Abdesslem, Shiva Nejati, Lionel C. Briand, and Thomas Stifter. 2018. Testing Vision-Based Control Systems Using Learnable Evolutionary Algorithms. In *International Conference on Software Engineering*. ACM, 1016–1026.
- [21] Alexander Boll, Florian Brokhausen, Tiago Amorim, Timo Kehler, and Andreas Vogelsang. 2021. Characteristics, potentials, and limitations of open-source Simulink projects for empirical research. *Software and Systems Modeling* 20, 6 (2021), 2111–2130.
- [22] Matteo Brunetto, Giovanni Denaro, Leonardo Mariani, and Mauro Pezzè. 2021. On introducing automatic test case generation in practice: A success story and lessons learned. *Journal of Systems and Software* 176 (2021), 110933.
- [23] Max H. Cohen and Calin Belta. 2021. Model-Based Reinforcement Learning for Approximate Optimal Control with Temporal Logic Specifications. In *International Conference on Hybrid Systems: Computation and Control*. ACM, 1–12.
- [24] Pouria Derakhshanfar, Xavier Devroey, Andy Zaidman, Arie van Deursen, and Annibale Panichella. 2020. Good Things Come In Threes: Improving Search-based Crash Reproduction With Helper Objectives. In *International Conference on Automated Software Engineering*. IEEE/ACM, 211–223.
- [25] DOE 2022 [Online]. United States Department of Energy. <https://www.energy.gov/>
- [26] Alexandre Donzé. 2010. Breach, A Toolbox for Verification and Parameter Synthesis of Hybrid Systems. In *Computer Aided Verification*. Springer, 167–170.
- [27] Alexandre Donzé and Oded Maler. 2010. Robust Satisfaction of Temporal Logic over Real-Valued Signals. In *Formal Modeling and Analysis of Timed Systems*. Springer, 92–106.
- [28] Driveline 2022 [Online]. Simscape Driveline Model and simulate rotational and translational mechanical systems. <https://www.mathworks.com/products/simscape-driveline.html>.
- [29] Pengfei Duan, Ying Zhou, Xufang Gong, and Bixin Li. 2018. A systematic mapping study on the verification of cyber-physical systems. *IEEE Access* 6 (2018), 59043–59064.
- [30] EcoCAR 2022 [Online]. The EcoCAR Mobility Challenge. <https://it.mathworks.com/academia/student-competitions/ecocar.html>.
- [31] Gidon Ernst, Sean Sedwards, Zhenya Zhang, and Ichiro Hasuo. 2018. Fast Falsification of Hybrid Systems using Probabilistically Adaptive Input. In *International Conference on Quantitative Evaluation of Systems*. Springer, 165–181.
- [32] Gidon Ernst, Sean Sedwards, Zhenya Zhang, and Ichiro Hasuo. 2021. Falsification of hybrid systems using adaptive probabilistic search. *Transactions on Modeling and Computer Simulation (TOMACS)* 31, 3 (2021), 1–22.
- [33] Gidon Ernst et al. Paolo Arcaini, Ismail Bennani, Aniruddh Chandratte, Alexandre Donzé, Georgios Fainekos, Goran Frehe, Khouloud Gaaloul, Jun Inoue, Tanmay Khandait, Logan Mathesen, Claudio Menghi, Giulia Pedrielli, Marc Pouzet, Masaki Waga, Shakiba Yaghoubi, Yoriyuki Yamagata, and Zhenya Zhang. 2021. ARCH-COMP Category Report: Falsification with Validation of Results. In *Workshop on Applied Verification of Continuous and Hybrid Systems*, Vol. 80. EasyChair, 133–152.
- [34] Georgios Fainekos, Bardh Hoxha, and Sriram Sankaranarayanan. 2019. Robustness of specifications and its applications to falsification, parameter mining, and runtime monitoring with S-TaLiRo. In *International Conference on Runtime Verification*. Springer, 27–47.
- [35] Georgios E Fainekos and George J Pappas. 2006. Robustness of temporal logic specifications. In *Formal Approaches to Software Testing and Runtime Verification*. Springer, 178–192.
- [36] Georgios E Fainekos and George J Pappas. 2009. Robustness of temporal logic specifications for continuous-time signals. *Theoretical Computer Science* 410, 42 (2009), 4262–4291. <https://doi.org/10.1016/j.tcs.2009.06.021>

- [37] Ansgar Fehnker and Franjo Ivančić. 2004. Benchmarks for hybrid systems verification. In *International Workshop on Hybrid Systems: Computation and Control*. Springer, 326–341.
- [38] Vahid Garousi, Michael Felderer, Çağrı Murat Karapıçak, and Uğur Yılmaz. 2018. Testing embedded software: A survey of the literature. *Information and Software Technology* 104 (2018), 14–45.
- [39] GM 2022 [Online]. General Motors. <https://www.gm.com/>.
- [40] GMD 2022 [Online]. General Motors recalling 4.3 million vehicles for airbag defect. <https://www.cbc.ca/news/business/general-motors-recall-airbag-software-1.3755030>.
- [41] Iman Haghighi, Noushin Mehdipour, Ezio Bartocci, and Calin Belta. 2019. Control from Signal Temporal Logic Specifications with Smooth Cumulative Quantitative Semantics. In *Conference on Decision and Control*. IEEE, 4361–4366.
- [42] M. Harman and J. Clark. 2004. Metrics are fitness functions too. In *International Symposium on Software Metrics*. IEEE, 58–69.
- [43] Mark Harman, Yue Jia, and Yuanyuan Zhang. 2015. Achievements, Open Problems and Challenges for Search Based Software Testing. In *International Conference on Software Testing, Verification and Validation*. IEEE, 1–12.
- [44] Emma Hart and Peter Ross. 2001. Gavel-a new tool for genetic algorithm visualization. *Transactions on Evolutionary Computation* 5, 4 (2001), 335–348.
- [45] Honda 2022 [Online]. Honda recalls 1.4M U.S. vehicles for software, other problems. <https://www.nbcnews.com/business/consumer/honda-recalls-1-4m-u-s-vehicles-software-other-problems-n1251496>.
- [46] Dmytro Humeniuk, Giuliano Antoniol, and Foutse Khomh. 2021. Data Driven Testing of Cyber Physical Systems. In *International Workshop on Search-Based Software Testing*. IEEE/ACM, 16–19.
- [47] Xiaoqing Jin, Jyotirmoy V Deshmukh, James Kapinski, Koichi Ueda, and Ken Butts. 2014. Powertrain control verification benchmark. In *International conference on Hybrid systems: computation and control*. ACM, 253–262.
- [48] James Kapinski, Jyotirmoy V Deshmukh, Xiaoqing Jin, Hisahiro Ito, and Ken Butts. 2016. Simulation-based approaches for verification of embedded control systems: An overview of traditional and advanced modeling, testing, and verification techniques. *IEEE Control Systems Magazine* 36, 6 (2016), 45–64.
- [49] Maria Kechagia, Xavier Devroey, Annibale Panichella, Georgios Gousios, and Arie van Deursen. 2019. Effective and Efficient API Misuse Detection via Exception Propagation and Search-Based Testing. In *International Symposium on Software Testing and Analysis*. ACM SIGSOFT, 192–203.
- [50] Manju Khari and Prabhat Kumar. 2019. An extensive evaluation of search-based software testing: a review. *Soft computing* 23, 6 (2019), 1933–1946. <https://doi.org/10.1007/s00500-017-2906-y>
- [51] Yong-Hyuk Kim and Byung-Ro Moon. 2002. Visualization of the fitness landscape, A steady-state genetic search, and schema traces. In *Annual Conference on Genetic and Evolutionary Computation*. Morgan Kaufmann, 686–686.
- [52] Yong-Hyuk Kim and Byung-Ro Moon. 2003. New usage of Sammon’s mapping for genetic visualization. In *Genetic and Evolutionary Computation Conference*. Springer, 1136–1147.
- [53] Florian Klück, Martin Zimmermann, Franz Wotawa, and Mihai Nica. 2019. Performance Comparison of Two Search-Based Testing Strategies for ADAS System Validation. In *International Conference on Testing Software and Systems*. Springer, 140–156.
- [54] LandRover 2022 [Online]. Software bug causes Land Rover recall. <https://www.themanufacturer.com/articles/almost-36500-jlr-vehicles-recalled-in-china/>.
- [55] Grisca Liebel, Nadja Marko, Matthias Tichy, Andrea Leitner, and Jörgen Hansson. 2018. Model-based engineering in the embedded systems domain: an industrial survey on the state-of-practice. *Software and Systems Modeling* 17, 1 (2018), 91–113. <https://doi.org/10.1007/s10270-016-0523-3>
- [56] Lars Lindemann and Dimos V. Dimarogonas. 2019. Robust control for signal temporal logic specifications using discrete average space robustness. *Automatica* 101 (2019), 377–387.
- [57] John J Majikes, Rahul Pandita, and Tao Xie. 2013. Literature review of testing techniques for medical device software. In *Medical Cyber-Physical Systems Workshop*. Citeseer.
- [58] Oded Maler and Dejan Nickovic. 2004. Monitoring temporal properties of continuous signals. In *Formal Techniques, Modelling and Analysis of Timed and Fault-Tolerant Systems*. Springer, 152–166.
- [59] Logan Mathesen, Shakiba Yaghoubi, Giulia Pedrielli, and Georgios Fainekos. 2019. Falsification of Cyber-Physical Systems with Robustness Uncertainty Quantification Through Stochastic optimization with Adaptive Restart. In *International Conference on Automation Science and Engineering*. IEEE, 991–997.
- [60] MathWorks 2022 [Online]. MathWorks. <https://www.mathworks.com>.
- [61] Reza Matinnejad, Shiva Nejati, Lionel Briand, and Thomas Bruckmann. 2014. MiL Testing of Highly Configurable Continuous Controllers: Scalable Search Using Surrogate Models. In *International Conference on Automated Software Engineering*. ACM/IEEE, 163–174.
- [62] Reza Matinnejad, Shiva Nejati, Lionel Briand, Thomas Bruckmann, and Claude Poull. 2015. Search-based automated testing of continuous controllers: Framework, tool support, and case studies. *Information and Software Technology* 57 (2015), 705–722. <https://doi.org/10.1016/j.infsof.2014.05.007>
- [63] Reza Matinnejad, Shiva Nejati, Lionel C. Briand, and Thomas Bruckmann. 2016. Automated Test Suite Generation for Time-Continuous Simulink Models. In *International Conference on Software Engineering*. ACM/IEEE, 595–606.
- [64] Reza Matinnejad, Shiva Nejati, Lionel C Briand, and Thomas Bruckmann. 2016. Automated test suite generation for time-continuous simulink models. In *International Conference on Software Engineering*. ACM, 595–606.
- [65] John H McDonald. 2009. *Handbook of biological statistics*. Vol. 2.
- [66] Noushin Mehdipour, Cristian-Ioan Vasile, and Calin Belta. 2019. Arithmetic-Geometric Mean Robustness for Control from Signal Temporal Logic Specifications. In *American Control Conference*. IEEE, 1690–1695.
- [67] Claudio Menghi, Shiva Nejati, Lionel Briand, and Yago Isasi Parache. 2020. Approximation-Refinement Testing of Compute-Intensive Cyber-Physical Models: An Approach Based on System Identification. In *International Conference on Software Engineering*. IEEE/ACM, 372–384.
- [68] Claudio Menghi, Shiva Nejati, Khouloud Gaoloul, and Lionel C Briand. 2019. Generating automated and online test oracles for simulink models with continuous and uncertain behaviors. In *joint meeting on european software engineering conference and symposium on the foundations of software engineering*. ACM, 27–38.
- [69] Andrew L. Nelson, Gregory J. Barlow, and Leferis Doitsidis. 2009. Fitness functions in evolutionary robotics: A survey and analysis. *Robotics and Autonomous Systems* 57, 4 (2009), 345–370. <https://doi.org/10.1016/j.robot.2008.09.009>
- [70] Truong Nghiem, Sriram Sankaranarayanan, Georgios Fainekos, Franjo Ivancić, Aarti Gupta, and George J Pappas. 2010. Monte-carlo techniques for falsification of temporal properties of non-linear hybrid systems. In *International conference on Hybrid systems: computation and control*. ACM, 211–220.
- [71] Annibale Panichella, Carol V. Alexandru, Sebastiano Panichella, Alberto Bacchelli, and Harald C. Gall. 2016. A Search-Based Training Algorithm for Cost-Aware Defect Prediction. In *Genetic and Evolutionary Computation Conference*. ACM, 1077–1084.
- [72] Annibale Panichella, Fitsum Meshesha Kifetew, and Paolo Tonella. 2018. Automated Test Case Generation as a Many-Objective Optimisation Problem with Dynamic Selection of the Targets. *IEEE Transactions on Software Engineering* 44, 2 (2018), 122–158. <https://doi.org/10.1109/TSE.2017.2663435>
- [73] Yash Vardhan Pant, Houssam Abbas, and Rahul Mangharam. 2017. Smooth operator: Control using the smooth robustness of temporal logic. In *Conference on Control Technology and Applications*. IEEE, 1235–1240.
- [74] PCHIP 2022 [Online]. Piecewise Cubic Hermite Interpolating Polynomial (PCHIP). <https://it.mathworks.com/help/matlab/ref/pchip.html>.
- [75] Hartmut Pohlheim. 1999. Visualization of evolutionary algorithms-set of standard techniques and multidimensional visualization. In *Genetic and Evolutionary Computation Conference*. Vol. 1. 533–540.
- [76] Zahra Ramezani, Alexandre Donzé, Martin Fabian, and Knut Åkesson. 2021. Temporal logic falsification of cyber-physical systems using input pulse generators. *EPIC Series in Computing* 80 (2021), 195–202.
- [77] Recall-problem 2022 [Online]. The auto industry’s growing recall problem—and how to fix it. https://www.alixpartners.com/media/14438/ap_auto_industry_recall_problem_jan_2018.pdf.
- [78] Recalls 2022 [Online]. The Current State of Automotive Software Related Recalls. <https://sibros.medium.com/the-current-state-of-automotive-software-related-recalls-ef5ca95a88e2>.
- [79] Zahra Sadri-Moshkenani, Justin Bradley, and Gregg Rothermel. 2022. Survey on test case generation, selection and prioritization for cyber-physical systems. *Software Testing, Verification and Reliability* 32, 1 (2022), e1794.
- [80] Omur Sahin and Bahriye Akay. 2016. Comparisons of metaheuristic algorithms and fitness functions on software test data generation. *Applied Soft Computing* 49 (2016), 1202–1214. <https://doi.org/10.1016/j.asoc.2016.09.045>
- [81] Alireza Salahi, Hussein Almulla, and Gregory Gay. 2020. Choosing the fitness function for the job: Automated generation of test suites that detect real faults. *Software Testing, Verification and Reliability* 30, 7–8 (2020). <https://doi.org/10.1002/stvr.1758>
- [82] Sriram Sankaranarayanan and Georgios Fainekos. 2012. Simulating insulin infusion pump risks by in-silico modeling of the insulin-glucose regulatory system. In *International Conference on Computational Methods in Systems Biology*. Springer, 322–341.
- [83] Simscape 2022 [Online]. Simscape Model and simulate multidomain physical systems. <https://www.mathworks.com/products/simscape.html>.
- [84] SimscapeElectrical 2022 [Online]. Simscape Electrical Model and simulate electronic, mechatronic, and electrical power systems. <https://www.mathworks.com/products/simscape-electrical.html>.
- [85] Simulink 2022 [Online]. Simulate a Simulink model. <https://it.mathworks.com/help/simulink/slrref/sim.html>.
- [86] Stateflow 2022 [Online]. Model and simulate decision logic using state machines and flow charts. <https://www.mathworks.com/products/stateflow>.
- [87] StellantisDefects 2022 [Online]. Stellantis recalls 370,000 Ram, Dodge vehicles; Ford recalls 150,000 F-150s. <https://www.autonews.com/regulation-safety/stellantis-recalls-370000-ram-dodge-vehicles-ford-recalls-150000-f-150s>.

- [88] TeslaCrash 2022 [Online]. A Tesla driver is charged in a crash involving Autopilot that killed 2 people. <https://www.npr.org/2022/01/18/1073857310/tesla-autopilot-crash-charges>.
- [89] TeslaDefects 2022 [Online]. Tesla recalls over 26K U.S. vehicles over software problem. <https://globalnews.ca/news/8605915/tesla-recall-software-problem/>.
- [90] Cumhur Erkan Tuncali, Bardh Hoxha, Guohui Ding, Georgios Fainekos, and Sriram Sankaranarayanan. 2018. Experience report: Application of falsification methods on the UxAS system. In *NASA Formal Methods Symposium*. Springer, 452–459.
- [91] Uber 2022 [Online]. How terrible software design decisions led to Uber’s deadly 2018 crash. <https://arstechnica.com/cars/2019/11/how-terrible-software-design-decisions-led-to-ubers-deadly-2018-crash/>.
- [92] Peter Varnai and Dimos V. Dimarogonas. 2020. On Robustness Metrics for Learning STL Tasks. In *American Control Conference*. IEEE, 5394–5399.
- [93] Masaki Waga. 2020. Falsification of Cyber-Physical Systems with Robustness-Guided Black-Box Checking. In *International Conference on Hybrid Systems: Computation and Control*. ACM, Article 11, 13 pages.
- [94] Masaki Waga. 2020. Falsification of cyber-physical systems with robustness-guided black-box checking. In *International Conference on Hybrid Systems: Computation and Control*. ACM, 11:1–11:13.
- [95] Josh L. Wilkerson and Daniel R. Tauritz. 2011. A Guide for Fitness Function Design. In *Annual Conference Companion on Genetic and Evolutionary Computation*. ACM, 123–124.
- [96] Xiong Xu, Li Jiao, and Ziming Zhu. 2018. A dynamic fitness function for search based software testing. In *Genetic and Evolutionary Computation Conference Companion*. IEEE, 320–321.
- [97] Yoriyuki Yamagata, Shuang Liu, Takumi Akazaki, Yihai Duan, and Jianye Hao. 2021. Falsification of cyber-physical systems using deep reinforcement learning. *IEEE Transactions on Software Engineering* 47, 12 (2021), 2823–2840. <https://doi.org/10.1109/TSE.2020.2969178>
- [98] Zhenya Zhang, Deyun Lyu, Paolo Arcaini, Lei Ma, Ichiro Hasuo, and Jianjun Zhao. 2021. Effective Hybrid System Falsification Using Monte Carlo Tree Search Guided by QB-Robustness. In *Computer Aided Verification*. Springer, 1–24.
- [99] Xin Zhou, Xiaodong Gou, Tingting Huang, and Shunkun Yang. 2018. Review on testing of cyber physical systems: Methods and testbeds. *IEEE Access* 6 (2018), 52179–52194.